Journal of Inorganic Biochemistry 183 (2018) 84–93

Contents lists available at ScienceDirect

Journal of Inorganic Biochemistry

journal homepage: www.elsevier.com/locate/jinorgbio

# Side chain removal from corticosteroids by unspecific peroxygenase

René Ullrich[a,1], Marzena Poraj-Kobielska[a,1], Steffi Scholze[a], Claire Halbout[b], Martin Sandvoss[b], Marek J. Pecyna[a,c], Katrin Scheibner[d], Martin Hofrichter[a,*]

[a] TU Dresden, International Institute Zittau, Department of Bio- and Environmental Sciences, Markt 23, 02763 Zittau, Germany
[b] Sanofi-Aventis Deutschland GmbH, R&D, Integrated Drug Discovery IDD, Isotope Chemistry & Metabolite Synthesis ICMS, G876, 65926 Frankfurt, Hoechst, Germany
[c] University of Applied Sciences Zittau-Görlitz, Faculty of Natural and Environmental Sciences, Theodor-Körner-Allee 16, 02763 Zittau, Germany
[d] BTU Cottbus-Senftenberg, Faculty of Environment and Natural Sciences, Universitätsplatz 1, 01968 Senftenberg, Germany

ARTICLE INFO

*Keywords:*
Peroxygenation
Peroxide shunt
P450
Heme-thiolate
Deacylation
Geminal alcohol

ABSTRACT

Two unspecific peroxygenases (UPO, EC 1.11.2.1) from the basidiomycetous fungi *Marasmius rotula* and *Marasmius wettsteinii* oxidized steroids with hydroxyacetyl and hydroxyl functionalities at C17 - such as cortisone, Reichstein's substance S and prednisone - via stepwise oxygenation and final fission of the side chain. The sequential oxidation started with the hydroxylation of the terminal carbon (C21) leading to a stable geminal alcohol (e.g. cortisone 21-*gem*-diol) and proceeded via a second oxygenation resulting in the corresponding α-ketocarboxylic acid (e.g. cortisone 21-oic acid). The latter decomposed under formation of adrenosterone (4-androstene-3,11,17-trione) as well as formic acid and carbonic acid (that is in equilibrium with carbon dioxide); fission products comprising two carbon atoms such as glycolic acid or glyoxylic acid were not detected. Protein models based on the crystal structure data of *Mro*UPO (*Marasmius rotula* unspecific peroxygenase) revealed that the bulky cortisone molecule suitably fits into the enzyme's access channel, which enables the heme iron to come in close contact to the carbons (C21, C20) of the steroidal side chain. ICP-MS analysis of purified *Mro*UPO confirmed the presence of magnesium supposedly stabilizing the porphyrin ring system.

## 1. Introduction

Steroidal compounds influence animals and humans in various ways [1,2]. They comprise several biologically active classes of substances such as bile acids, cardio-active drugs (cardiotonics), steroid sapogenins, steroid alkaloids as well as sexual and corticosteroidal hormones [3]. As hormones, they regulate metabolic and ontogenetic processes in humans from fetal life to adulthood. Because of their biological effects, steroids are not only of general scientific interest but also of medical relevance, not least with respect to pharmaceutical applications. In animals including humans, steroids are made from lanosterol that derives from cyclization of the triterpene squalene, which for its part is a product of the mevalonate pathway [4]. One group of pharmaceutically relevant steroids are C21 hormones (pregnane core), which include gluco- and mineralocorticoids produced in the adrenal cortex as well as their precursor progesterone. The latter can be transformed via hydroxylation to 17α-hydroxy progesterone and subsequent side chain removal or C21 hydroxylation to androstenedione and 11-deoxycortisol (Reichstein's substance S), respectively; the former is the direct precursor of the male sexual hormone testosterone and the latter of the glucocorticoid cortisol. Both Reichstein's substance S and androstenedione are important intermediates in industrial steroid syntheses.

Steroids used for therapeutic or other pharmaceutical purposes are largely products of partial synthesis starting from animal cholesterol or herbal phytosterols or sapogenins. The addition, removal and modification of functional groups to, from and at these starting materials is of central importance when producing the wide variety of steroidal drugs. These modifications are achieved using conventional organic synthesis and/or microbial whole-cell biotransformations [5,6]. Cytochrome P450 enzymes (P450s, CYPs) are the key biocatalysts of steroid biotransformation and catalyze hydroxylation, epoxidation, aromatization and side chain removal [2]. Such reactions are integral part of steroid biosynthesis pathways in humans and animals (see above) and some of them can be also found in microorganisms (fungi, bacteria); typically in form of single transformations with often unknown function for the microbes (e.g. 11α-, 11β- and 16α-hydroxylation by *Bacillus*, *Mycobacterium*, *Curvularia* or *Cunninghamella*) [6,7]. However, microbial systems do not mimic all relevant human steroid transformations. Thus side-chain removal (C—C bond cleavage) from

* Corresponding author.
*E-mail address:* martin.hofrichter@tu-dresden.de (M. Hofrichter).
[1] These authors contributed equally to this work.

https://doi.org/10.1016/j.jinorgbio.2018.03.011
Received 13 March 2018; Accepted 22 March 2018
Available online 26 March 2018

progesterone or pregnenolone is exclusively accomplished by vertebrate CYP17A1 (also known as a 17α-hydroxylase/17,20-lyase). It proceeds through two intrinsic reactions: in the first one, the enzyme hydroxylates the 17α-position and in the second reaction, it cleaves the C−C bond between C17 and C20 in a lyase-like reaction resulting in the release of acetate [8]. To our best knowledge, however, steroids hydroxylated in position C21 such as Reichstein's substance S, cortisol or cortisone are not subject of C-C cleavage by CYP17A1 or any microbial P450. Since, on the other hand, Reichstein's substance S is a key precursor in industrial steroid syntheses [9], it would be worthwhile to have a catalyst that selectively removes the respective hydroxyacetyl moiety to form the corresponding keto-derivatives (17-ones).

Unspecific peroxygenase (UPO, EC 1.11.2.1) is a secreted fungal enzyme type that efficiently transfers oxygen from peroxides (R-OOH) to diverse substrates including unactivated hydrocarbons [10]. Literally, such enzymes strictly follow the peroxide “shunt” pathway of P450s and in this context, they can reach total turnovers numbers of $10^4$ to almost $10^6$ for oxygen transfer reactions [11–13]. As P450s, UPO enzymes are heme-thiolate proteins but they do not share any sequence homology with them. Highest sequence homology has been ascertained to fungal chloroperoxidase (CPO, EC 1.11.1.6) that is actually a UPO with strong halide oxidation activity [14]. Among the UPO-catalyzed reactions are hydroxylations, epoxidations, *O*- and *N*-dealkylations, oxidations of organic hetero atoms and bromide as well as one-electron oxidations. Their catalytic cycle involves formation of a highly reactive oxoferryl intermediate (compound I) and a protonated basic compound II (oxoferryl hydroxide) that are the active oxygen species in hydroxylation reactions [15,16]. Crystal structure of the UPO from *Agrocybe aegerita* (*Aae*UPO) was solved and has given first insights into the molecular organization of this exceptional peroxidase type [17,18].

Here we report two UPOs from the mushrooms *Marasmius rotula* (*Mro*UPO) [19] and *Marasmius wettsteinii* (*Mwe*UPO, novel wild-type UPO first described herein), which catalyze the selective deacylation of 17α,21-dihydroxycorticosteroids. To our best knowledge, this reaction has not been reported so far for any microbial P450 and represents a new reaction type for UPOs.

## 2. Materials and methods

### 2.1. Chemicals

Formic acid (pro analysis) and acetonitrile (ACN, gradient grade for liquid chromatography) were purchased from VWR (Darmstadt, Germany). All other chemicals including cortisone (S I), prednisone (S II), Reichstein's substance S (S III), and adrenosterone (P III) were obtained from Sigma-Aldrich GmbH (Schnelldorf, Germany) in the highest available purity.

### 2.2. Enzyme preparation and characterization

The extracellular peroxygenases from the basidiomycetous fungi *Agrocybe aegerita* (*Aae*UPO; main isoform, 46 kDa) and *Marasmius rotula* (*Mro*UPO; main isoform, 32 kDa denaturated and 58 kDa native) were produced and purified as described previously [19,20]. The enzyme preparations were homogeneous according to sodium dodecyl polyacrylamide gel electrophoresis (SDS-PAGE) and analytical high performance liquid chromatography-size exclusion chromatography (HPLC-SEC). The specific activities of the *Aae*UPO and *Mro*UPO preparations were 99.6 U mg$^{-1}$ and 26.0 U mg$^{-1}$, respectively. One unit (1 U) corresponds to the oxidation of 1 μmol of veratryl alcohol (3,4-dimethoxybenzyl alcohol) to veratraldehyde (3,4-dimethoxybenzaldehyde) in 1 min at 23 °C [20]; activity measurements were performed in 50 mM sodium phosphate buffer at pH 7.0 (*Aae*UPO) or 5.5 (*Mro*UPO and *Mwe*UPO).

A novel wild-type peroxygenase was produced with *Marasmius wettsteinii* (*Mwe*UPO) strain 582 deposited at the culture collection of the International Institute Zittau (Technical University of Dresden, Germany) and at DSMZ Braunschweig (*Deutsche Stammsammlung für Mikroorganismen und Zellkulturen*, Germany) under DSM 106021. The fungus was isolated from fruiting bodies growing on spruce needle litter (*Picea abies*) near the Kottmar mountain in East Saxony (Germany) in September 2015 (more information on the fungal species is given in the Supplemental Information section). Stock cultures were maintained in culture slants on 2% malt extract agar at 4 °C in the dark. For enzyme production, the content of a completely overgrown agar-plate was homogenized in 80 mL sterile tap water and used for the inoculation of liquid cultures (5% vol/vol of the suspension). Submerged cultivation was performed in 500-mL Erlenmeyer flasks containing 200 mL of a complex liquid medium according to Gröbe et al. [19] on a rotary shaker (120 rpm, at 23 °C). The time course of *Mwe*UPO production is shown in Fig. S1. Fungal cultures were harvested after three weeks when the UPO activity had reached approximately 2500 U L$^{-1}$. Crude extracts of concentrated culture liquid contained at least five isoforms of *Mwe*UPO. The major isoform was isolated via different steps of fast protein liquid chromatography (FPLC) and had a final specific activity of 37.5 U mg$^{-1}$; the corresponding purification table is given in Table S1. Homogeneity of the final *Mwe*UPO preparation was proven by SDS-PAGE and HPLC-SEC and compared to *Mro*UPO and *Aae*UPO (Fig. S2 and S3). Molecular mass of the native enzyme was 62 kDa (determined by HPLC-SEC; Fig. S2) and 32.5 kDa according to denaturing SDS-PAGE (Fig. S3) indicating, as in the case of *Mro*UPO, a physiological dimer [21]. HPLC-SEC of purified *Mwe*UPO was carried out using an Agilent Series 1200 instrument equipped with a diode array detector (Agilent Technologies Deutschland GmbH, Waldbronn, Germany) and a Yarra 3 μ SEC-2000 column (300 × 7.8 mm, Phenomenex, Aschaffenburg, Germany). Separation of UPO proteins was achieved at 25 °C under isocratic conditions (flow rate 1 mL min$^{-1}$) with sodium acetate/sodium chloride (50 mM/100 mM, pH 6.9) as eluent. Calibration occurred with a gel filtration low-molecular weight calibration kit from GE Healthcare (Munich, Germany). SDS-PAGE was performed as described previously [22].

### 2.3. Enzymatic reaction setup

Typical reaction set-ups (0.2–1.0 mL) contained UPO protein (1.0–2.0 U mL$^{-1}$ corresponding to 0.04–0.08 μM = 0.014–0.028 mg mL$^{-1}$), 0.5–2.0 mM steroidal substrate (stock solution in 50% ACN resulting in a final ACN concentration of 5 vol%) and 50 mM potassium phosphate buffer (pH 7.0 or 5.5). The reactions stirred at room temperature were started with $H_2O_2$ by either adding it directly (0.1 to 2 mM $H_2O_2$) or supplying it continuously with a syringe pump (0.5 mM h$^{-1}$ for 4 h). For kinetic studies, aliquots were taken from the reaction mixtures every 20 min and analyzed by high performance liquid chromatography-mass spectrometry (HPLC-MS).

The reaction setup was scaled up to 50 mL to separate and purify the products of enzymatic steroid conversion for subsequent NMR analysis. The reaction solution contained 20 U (5.6 μg mL$^{-1}$) of purified *Mro*UPO, 80 mg of the substrate (S I cortisone, S II prednisone or S III Reichstein's substance S; chemical structures are shown in Fig. 1), 2.5 mL of ACN (final concentration of 5% vo/vol) and potassium phosphate buffer (50 mM, pH 5.5). The reaction was started by the addition of hydrogen peroxide ($H_2O_2$, 1 mM) and repeated every 6 min over 1 h (final concentration 10 mM).

### 2.4. Analytical methods

#### 2.4.1. HPLC-MS method I (for standard reactions)

Products of enzymatic syntheses were analyzed by high performance liquid chromatography (HPLC) using an Agilent Series 1200 instrument equipped with a diode array detector and an electrospray ionization mass spectrometer (ESI-MS) (Agilent Technologies Deutschland GmbH, Waldbronn, Germany). Unless otherwise stated, reverse

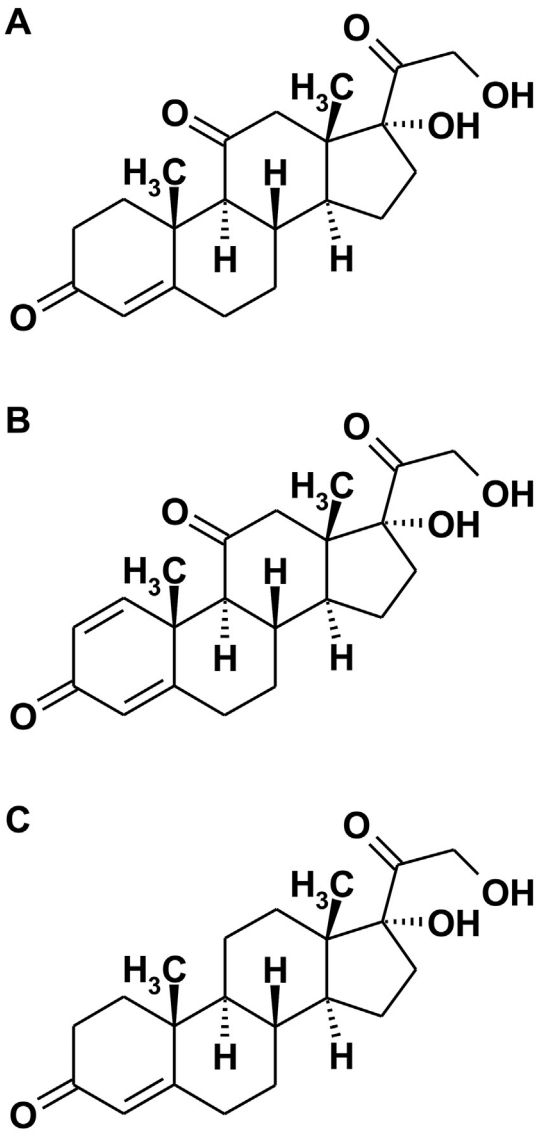


**Fig. 1.** Chemical structures of corticosteroids used in this study: S I cortisone (A), S II prednisone (B) and S III Reichstein's substance S (C).

phased chromatography on a Luna C18 column (2 mm diameter by 250 mm length, 3 µm particle size, Phenomenex, Aschaffenburg, Germany) was used. Column was eluted at a flow rate of 0.2 mL $min^{-1}$ and 40 °C with aqueous 0.01% vol/vol ammonium formate (pH 3.5)/ACN, 95:5 for 5 min, followed by a 15-min linear gradient to 100% ACN. Mass spectrometric measurements were made in positive or negative ESI mode in a mass range from 70 to 900, step size 0.1, drying gas temperature 350 °C, capillary voltage 4000 V for positive mode and 5500 V for negative mode. Reaction products were identified relative to authentic standards, based on their retention times, UV absorption spectra, and mass spectral data ([M + H] or [M − H] ions).

#### 2.4.2. HPLC-MS method II

Additional analyses were performed using a Kinetex C18 column (2 mm diameter by 250 mm length, 5 µm particle size, Phenomenex), which was eluted with a flow rate of 1 mL $min^{-1}$ at 40 °C with aqueous 0.01% vol/vol ammonium formate (pH 3.5)/ACN, 95:5 for 2 min, followed by a 12-min linear gradient to 100% ACN. MS parameters were the same as described under method I.

#### 2.4.3. HPLC-MS method III

Kinetic studies on the conversion of cortisone by *Mro*UPO and *Mwe*UPO were carried out by applying a more rapid HPLC method. Respective samples were analyzed using a Phenomenex Kinetex Phenyl-Hexyl column (2.6 µm particle size, 150 × 2.1 mm). The flow rate was 0.4 mL $min^{-1}$ and the temperature set to 40 °C. The following gradient of 0.01 vol% ammonium formate (pH 3.2) and ACN was performed: 0–0.2 min 20% ACN followed by a linear gradient to 65% ACN (0.2–10 min) and to 85% (10–12 min). The MS parameters were the same as in method I.

#### 2.4.4. Ion chromatography (IC) method for organic acids

Organic acids were analyzed by IC using a Dionex Series ICS1100 system (Thermo Fisher GmbH, Idstein, Germany) fitted with an IonPac® ICE-AS1 column (4 mm diameter by 250 mm length, Dionex, Germering, Germany). The column was eluted at 30 °C and 1.6 mL $min^{-1}$ with an aqueous perfluorobutyric acid solution (1 mM) over 20 min. Products were identified relative to the authentic standards by their retention times.

HPLC-UV method for organic acids. Analyses were performed using a Rezex™ ROA-Organic Acid $H^+$ (8%) column (7.8 mm diameter by 300 mm length, Phenomenex). The column was eluted at 50 °C and 0.5 mL $min^{-1}$ with an aqueous sulfuric acid solution (0.005 N) over 25 min. Acids were recorded at 210 nm and identified relative to authentic standards by their retention times.

### 2.5. Product isolation

Products of enzymatic steroid oxidation were separated and purified by preparative HPLC using a 1260 Infinity Agilent system (Agilent Technologies Deutschland GmbH) equipped with a Kinetex C18 column (Axia packed, 21.2 mm diameter by 150 mm length, 5 µm particle size, Phenomenex), which was eluted at 20 mL $min^{-1}$ and room temperature with water/ACN 70:30 for 1 min under isocratic conditions, followed by a 5-min linear gradient to 70% ACN and a 1.5-min gradient to 100% CAN, which was hold for 0.5 min and then set to 30% ACN within 1 min. Eluting peaks (detected at 240 nm) were sampled with an Infinity fraction collector (fraction collector; preparative scale, G1364B, Agilent Technologies Deutschland GmbH). The purity of isolated products was checked by analytical HPLC-MS (method I above).

### 2.6. NMR spectroscopy experimental conditions

2.65 mg of P I and 0.5 mg of P II were transferred into capillary NMR tubes of 2.5 × 100 mm in 150 µL dimethylsulfoxide-d6 (99.8%, Deutero, Kastellaun, Germany). Proton, COSY (correlated spectroscopy), HSQC (heteronuclear single quantum coherence) and HMBC (heteronuclear multiple bond correlation) spectra were recorded on a Bruker Avance 500 MHz spectrometer equipped with a 2.5 mm selective inverse SEI probe (Bruker, Rheinstetten, Germany). For technical reasons, some HMBC spectra had to be recorded on a Bruker Avance III 600 MHz instrument equipped with a 1.7 mm inverse SEI probe (part of the sample was transferred in to 1.7 × 100 mm microtubes). For chemical shift prediction, the ACD/C + H NMR predictors, release 2015, pack2, from ACDlabs (Toronto, Ontario, Canada) were used.

### 2.7. Precipitation of carbon dioxide with barium hydroxide

Carbon dioxide ($CO_2$) formation in the course of side chain removal from cortisone was qualitatively proved in a separate experiment. Two vials filled with 1 mL of saturated barium hydroxide [$Ba(OH)_2$] were connected via silicon tubes with two further vials containing the reaction mixture with *Mro*UPO (active sample) or a control without enzyme (Fig. S7). The reaction occurred under helium atmosphere. Before starting the reaction, the intrinsic $CO_2$ was stripped by flushing with helium, over 10 min. Afterwards the reaction was started as described

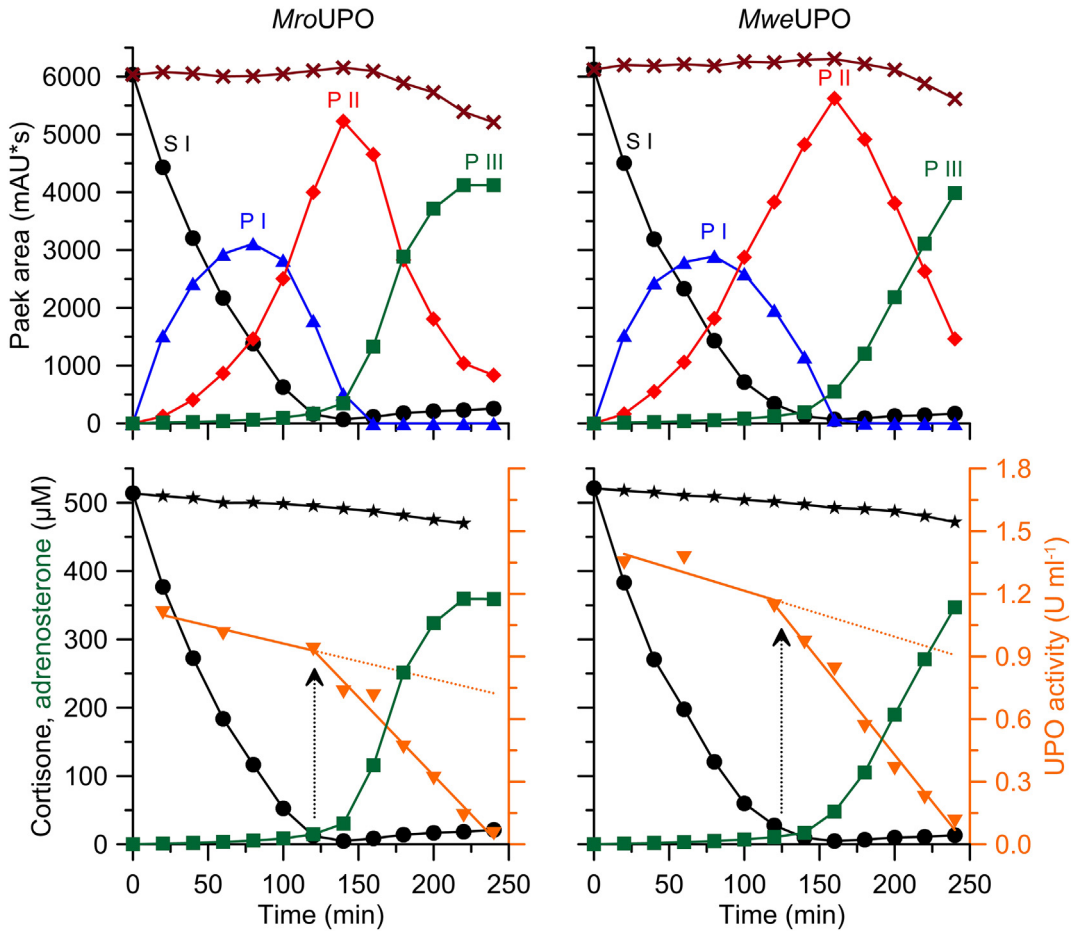


**Fig. 2.** Time courses of the conversion of cortisone by *Mro*UPO and *Mwe*UPO. Analyses were carried out by HPLC at 240 nm. Data are given in mAU*s of the respective peak areas (top) and in μM (bottom) along with the residual UPO activities (bottom). Black circles - cortisone (S I), blue up-pointing triangles - product P I (cortisone 21-*gem*-diol, *m/z* 376), red diamonds - product P II (cortisone 21-oic acid, m/z 374), green squares - product P III (adrenosterone, m/z 300), brown crosses - sum of peak areas, black asterisks - cortisone (S I) control, orange down- pointing triangles - residual UPO activity. Arrows mark the point of complete substrate consumption (S I, cortisone). Reaction solutions contained 1 U $mL^{-1}$ UPO, 0.5 mM cortisone (S I) in 10 mM potassium phosphate buffer (pH 5.5). $H_2O_2$ was supplied by syringe pump at 0.5 mM $h^{-1}$. (For interpretation of the references to colour in this figure legend, the reader is referred to the web version of this article.)

above but under continuous bubbling of helium through the vials. The stripped gaseous compounds were transferred into the $Ba(OH)_2$ vials where the $CO_2$ was trapped as insoluble barium carbonate ($BaCO_3$; compare Fig. S7).

### 2.8. Determination of the metal content in MroUPO

Purified *Mro*UPO was washed with deionized water resulting in a final protein concentration of 4 μM determined by a standard Bradford assay. Inductively coupled plasma optical emission spectroscopy (ICP-OES) and ICP mass spectrometry (ICP-MS) were performed on an Optima 3000 system and an Elas DRC-e device (both PerkinElmer Inc., MA, USA), respectively. The OES-system was calibrated with the 'ICP multi-element standard solution IV' (Mg, K, Ca, Mn, Fe, Cu) as well as the 'phosphorus ICP standard' (both Merck, Darmstadt, Germany) in 1 mg $L^{-1}$ and 10 mg $L^{-1}$ concentrations. Deionized water served as enzyme blank solution. Measurements were performed according to the manufacturers' specifications. Different concentrations (2, 15, and 50 μg $L^{-1}$) of the 'ICP multi-element standard solution VI' (V, Mn, Fe, Co, Cu; Merck, Darmstadt, Germany) were used to calibrate the MS unit.

### 2.9. Crystal structure and 3D-modelling

The crystal structure data of *Mro*UPO have been made available recently (protein data bank entries 5FUJ and 5FUK). Based on them, first structures were published indicating that *Mro*UPO is a dimeric protein with a relatively wide heme access channel [21]. Cortisone was docked into the *Mro*UPO active site cleft using the open-source program AutoDock Vina, version 1.1.2 [23]. The *Mro*UPO structure (PDB 5FUJ) and the cortisone molecule (3D conformation obtained from PubChem [24], CID 222786; 4 rotatable bonds) were prepared for docking in AutoDockTools [25], version 1.5.6. In order to define the active site of *Mro*UPO, cortisone as substrate was first placed manually at the entrance of the protein's binding pocket using PyMOL (The PyMOL Molecular Graphics System, Version 2.0 Schrödinger, LLC). The grid box was centered at x: −10.607, y: −17.81 and z: −28.584 with sizes of 20.25, 16.5, and 9.75 Å, respectively. Exhaustiveness was tested between 8 and 100. No more than twenty output poses (energy range 5 kcal $mol^{-1}$ with a maximum number of 30 for binding modes) were generated. In separated runs, the best three models occurred repeatedly. The docking model with highest affinity (−8.3 kcal $mol^{-1}$) in all runs shows close proximity of cortisone C21 to heme iron (4.4 Å) and is shown in Fig. 6.

## 3. Results

### 3.1. Enzymatic conversion of cortisone (S I)

Both *Mro*UPO and *Mwe*UPO were found to be capable of converting

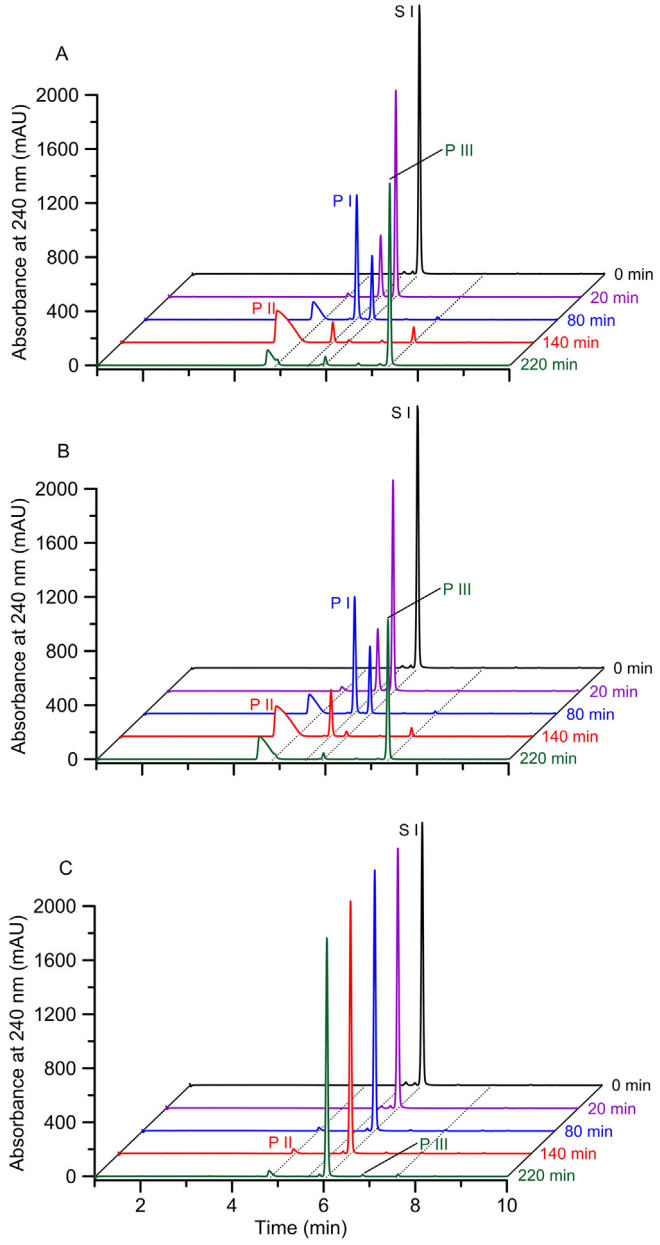


**Fig. 3.** HPLC elution profiles of reaction solutions containing cortisone (S I, 0.5 mM) and 1 U $mL^{-1}$ of three different UPOs; they were recorded after different reaction times (0–220 min). $H_2O_2$ was supplied by syringe pump at 0.5 mM $h^{-1}$ over the indicated time. A) *Mro*UPO, B) *Mwe*UPO and C) *Aae*UPO.

cortisone (S I, *m/z* M + $H^+$: 361) by almost 100%, while *Aae*UPO did not accept this compound as substrate. For the first 20 min of the reaction, we calculated turnover numbers (TON) of 6.4 $min^{-1}$ and 6.1 $min^{-1}$, respectively. These TON were limited by the limited amount of $H_2O_2$ gently and continuously supplied via a syringe pump, which would theoretically entail a maximum TON of 6.9 $min^{-1}$ under the conditions applied (co-substrate limitation to prevent heme damage). The first product that appeared within 20 min had a molecular mass of 376 (P I; *m/z* M + $H^+$: 377) indicating a hydroxylated metabolite (Fig. 2). 20 min later, a second product was detectable with a molecular mass of 374 (P II; *m/z* M + $H^+$: 375) probably representing an oxidation product of P I. P II showed an unusual peak shape (tailing) in the HPLC elution profile that is characteristic for keto-enol tautomerism or the presence of an aldehyde hydrate (that is in equilibrium with the corresponding free aldehyde). After 80 min, the formation of P I had reached its maximum, while the peak of P II still increased. 160 min after starting the reaction, a third product (P III) emerged with a smaller mass of 300 (m/z M + $H^+$: 301); it was identified by means of an authentic standard as adrenosterone and simultaneously, P II started to decrease (Fig. 2). At the end of the experiment (after 220 min), only 20% of P II's maximum peak area remained, while P III reached a maximum concentration of 359 and 347 μM in the case of *Mro*UPO and *Mwe*UPO, respectively. The respective results are summarized in Figs. 2, 3 and S5. Compared to the *Marasmius* UPOs, *Aae*UPO merely converted S I to negligible extent (< 1%), which resulted in traces of P II and P III (Fig. 3).

The observed HPLC peak pattern and the almost identical UV spectra of substrate and products, caused by the unchanged chromophore (double bonds in the steroidal A ring), prompted us to analyze the MS data more in detail to identify possibly hidden additional products. Indeed, the hint of an additional mass eluting at the same time as the substrate (S I) was observed. Therefore, the HPLC method was modified and improved (among others by changing the stationary phase). Then, we analyzed the extracted ion counts of the respective MS data (given in Fig. S5 for *Mwe*UPO) again and found a fourth product (P IV; most likely 17-hydroxy-3,11-dioxoandrost-4-ene-17-carboxylic acid) with a molecular mass of 346 (*m/z* M + $H^+$: 347). Fig. S5 displays a further metabolite (P V) with a mass of 316 (m/z: 317 M + $H^+$), probably a hydroxylation product of the fission product P III. Both P IV and P V were only detectable in traces and could not be quantified because of lacking standards; thus changes in their concentration were deduced from the corresponding peak areas (based on UV-absorption).

### 3.2. NMR spectroscopic analysis of the products P I and P II

Particular efforts were made to unambitiously identify the products P I, P II and P III by $^{13}C/^{1}H$ NMR spectroscopy. The NMR assignment of P I was based on the analysis of the side chain resonances in conjunction with chemical shift prediction and comparison to cortisone reference spectra (Table S2). In the side chain, a CH signal at 84.1/5.39 ppm indicating an alcoholic substitution was observed along with a carbonyl function at 207.0 ppm. Two possible keto-enol tautomeric structures were considered. The COSY showed that the CH signal at 84.1/5.39 ppm couples to two OH doublets at 6.12 and 6.36 ppm, respectively. Moreover, we observed HMBC correlations between the carbonyl resonance at 207.0 ppm and the CH proton at 5.39 ppm and the OH protons at 6.12 and 6.36 ppm. Furthermore, we observed HMBC couplings between the carbon at 84.05 ppm and two OH (6.12 and 6.36 ppm). This clearly establishes P I to be structure 1 (cortisone 21-*gem*-diol) given in Fig. 4, along with an additional minor species in the same sample (P Ia accounting for approximately 14%). The structure of P Ia being the hydrate of an aldehyde prompted us to further inspect the heteronuclear spectra: Fig. 4 shows the aldehyde section of the respective HMBC spectrum. A correlation between a CH at 9.66/195.2 ppm (spread by its $^{1}J$ (C,H) coupling of 189 Hz) and a carbonyl C at 200.5 ppm (showing a $^{2}J$ (C,H) coupling of 27 Hz) indicates the presence of the free aldehyde P Ia (cortisone 21-al) in the sample (Fig. 4).

For the second metabolite (Table S3), P II, we suggest the structure of a carboxylic acid (cortisone 21-oic acid) given in Fig. 5. Inspection of the proton, COSY and HSQC spectra showed that the sterane scaffold resonances were unchanged, while side chain CH resonances could not be observed. An additional OH proton resonance appeared at 7.09 ppm (integral one proton). Unfortunately, the sample's concentration was too low to observe the carbonyl $^{13}C$ signals, through neither direct $^{13}C$ NMR nor HMBC.

P III was the major product at the end of the reaction (with about 70% yield) and identified as adrenosterone (4-androst-ene-3,11,17-trione) by means of an authentic standard. As the corresponding fission products, we found traces of formic acid (HCOOH) and carbonic acid ($H_2CO_3$) by ion chromatography (IC; data not shown) and HPLC with UV detection (Fig. S6). In addition, the formation of carbon dioxide

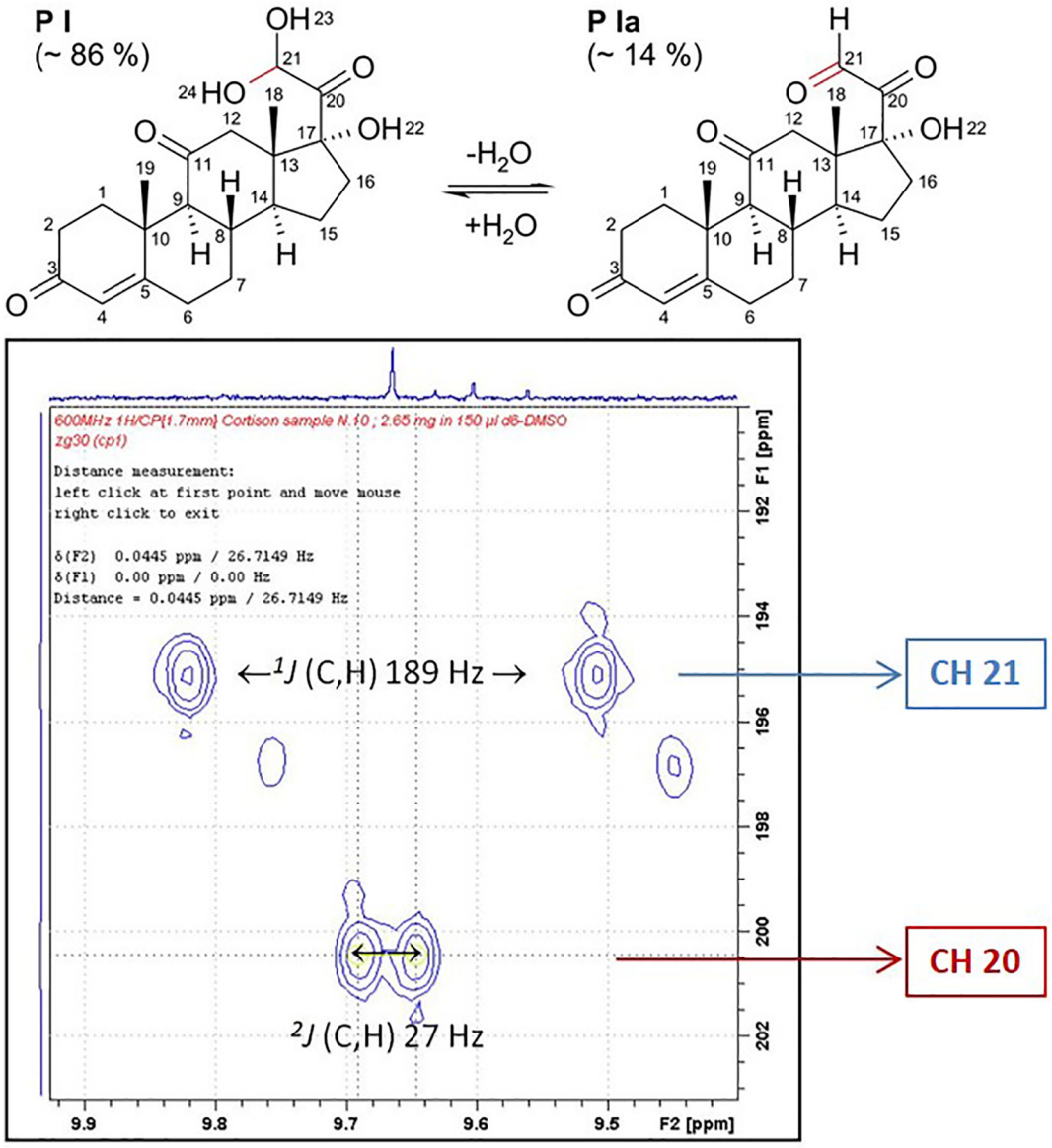


**Fig. 4.** Chemical structure of the cortisone metabolite P I with a molecular mass of 376.44 g mol$^{-1}$ and the molecular formula $C_{21}H_{28}O_6$ confirmed by NMR (left) as well as the corresponding dehydrated aldehyde P Ia being in equilibrium with P I. Bottom: HMBC spectrum of P I indicating the presence of the corresponding free aldehyde (P Ia).

(that is in equilibrium with carbonic acid and bicarbonate) in the reaction solution was confirmed by the formation of a whitish smear of precipitating barium carbonate ($BaCO_3$) when gaseous substances formed were stripped from the reaction solution and flushed through a barium hydroxide solution (Fig. S7). Unexpectedly, glycolic acid (HO-$H_2$C-COOH) and glyoxylic acid (OHC-COOH) – the supposed fission products – were not detectable in the reaction solutions. On the other hand, glycolic acid was found to be a substrate of *Mro*UPO that was rapidly oxidized into glyoxylic acid, formic acid and carbon dioxide as proved by HPLC-UV, IC and $BaCO_3$ formation (data not shown).

The residual UPO activity in the reaction solution followed an interesting biphasic time course (both for *Mro*UPO and *Mwe*UPO). As long as S I and P I were present in the reaction solution, the enzyme activity remained rather stable, however, after their consumption (between 120 and 140 min), the activity strongly decreased, probably caused by unfavorable catalysis during conversion of P II into the final product P III (Fig. 2).

The conversion of prednisone (S II) and Reichstein's substance S (S III) by *Mro*UPO and *Mwe*UPO gave similar results as for S I. Both compounds were converted in three ways following the mass changes $\Delta m/z = +16$, $\Delta m/z = +14$ and $\Delta m/z = -60$. The latter mass indicates that the last step was again a side chain removal resulting in the formation of 4-androsten-3,17-dione and 1,4-androstadien-3,11,17-trione, respectively (data not shown). *Aae*UPO oxidized S II and S III to negligible extent (< 1%) with traces of S (−60) as sole product.

### 3.3. Structure and metal content of MroUPO

Based on the recently published coordinates and first crystal structure of *Mro*UPO [21], we performed a docking analysis using cortisone (substrate S I) as ligand and *Mro*UPO as receptor with the open-source program AutoDock Vina. Corresponding Fig. 6 shows that the corticosteroid molecule almost perfectly fits into the active site of *Mro*UPO, while exposing the side chain to be removed towards the reactive heme center. In the computed model, cortisone's C21 appears in close proximity to the heme iron (4 Å). The binding pocket virtually consists just of aliphatic residues (leucine, Leu; isoleucine, Ile) and contains merely one aromatic residue (phenylalanine, Phe). One polar serine

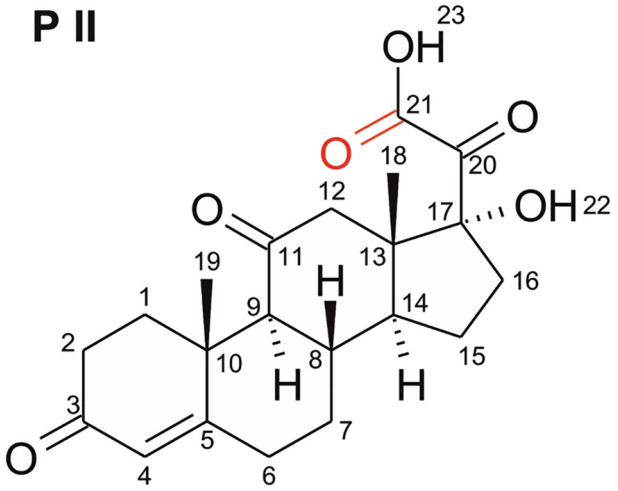


**Fig. 5.** Proposed structure of metabolite P II with a molecular mass of 374.43 g mol$^{-1}$ and following molecular formula: $C_{21}H_{26}O_6$.

residue (Ser156) is also found in this pocket; however, this residue does seemingly not form polar contacts to cortisone in the best fitting docking models. The keto groups at C3 and C11 of cortisone lie outside the binding pocket. The hydroxyl group at C17 as well as the keto group at C20 do not have polar contacts to amino acid residues of *Mro*UPO. In the second best fitting model (with correct orientation of the hydroxyacetyl group to heme but slightly less binding affinity of −8.2 kcal mol$^{-1}$), these both oxygen functionalities build intra-molecular contacts. The hydrogen of the hydroxyl group at C21 can build a polar contact to the hydroxyl-oxygen of the carboxylic group of a glutamate (Glu157, the distal acid-base catalyst) and thereby stabilizes correct substrate binding.

Since magnesium (Mg) had been found in the crystal structure of *Aae*UPO [18], we checked whether *Mro*UPO does also contain this probably stabilizing metal. ICP-MS and ICP-OES analyses in fact revealed that Mg was along iron (Fe) the most abundant metal in purified *Mro*UPO. Its amount corresponded to nearly one mol Mg per UPO molecule (Table S4). In contrast, the concentration of other metals, including manganese (Mn) and calcium (Ca) reported to be present in other heme peroxidases [26–28], were noticeably lower.

## 4. Discussion

Two UPOs from the mushroom genus *Marasmius* (*Mro*UPO, *Mwe*UPO) were found to convert corticosteroids with hydroxyacetyl (-CO-$CH_2$OH) and alcohol (-OH) functionalities at C17 via stepwise oxygenation/oxidation and final removal of the side chain (C-C cleavage, deacylation). In contrast, the model enzyme *Aae*UPO known to oxidize diverse other substrates, failed in catalyzing this reaction [10,29]. In a previous study, three UPOs including *Aae*UPO and *Mro*UPO were shown to hydroxylate steroids with longer side chains (with 8–10 carbon atoms) such as cholesterol, ergosterol and sitosterol preferably at tertiary C25, their scission, however, was not observed [30]. Another UPO from the ascomycetous mold *Chaetomium globosum* (*Cgl*UPO) has recently been demonstrated to selectively epoxidize (at 4,5-position) testosterone that is neither a substrate of *Mro*UPO nor of *Aae*UPO [31].

The ability of *Mro*UPO and *Mwe*UPO to convert bulky substrates such as cortisone (S I), prednisone (S II) and Reichstein's substance S (S III) can be attributed to the size and molecular architecture of the enzymes' active site. Both *Marasmius* enzymes belong to the cluster (subfamily) of “short” UPOs whereas *Aae*UPO is a “long” UPO that differs in several features from the former ones [29]. Thus, the heme access channel of *Mro*UPO is about 4 Å shorter and up to 5 Å wider than that of *Aae*UPO. Furthermore, the hydrophobic amino acid residues flanking the heme access channel are different. While *Aae*UPO contains nine rigid Phe and one Tyr forming a rather narrow “carafe-shaped” heme channel (Fig. 7B), *Mro*UPO's heme channel comprises only one Phe but ten more flexible aliphatic amino acids (1 Ala, 2 Leu, 7 Ile; Fig. 6) and thus forms a rather open and symmetric frustum (Fig. 7A) [18]. These structural differences may explain, which is why *Mro*UPO (and also *Mwe*UPO that shares > 90% sequence identity with *Mro*UPO, unpublished result) harbor and convert bulky substrates such as corticosteroids whereas *Aae*UPO cannot (Fig. 6).

A plausible reaction sequence involving the stepwise oxygenation

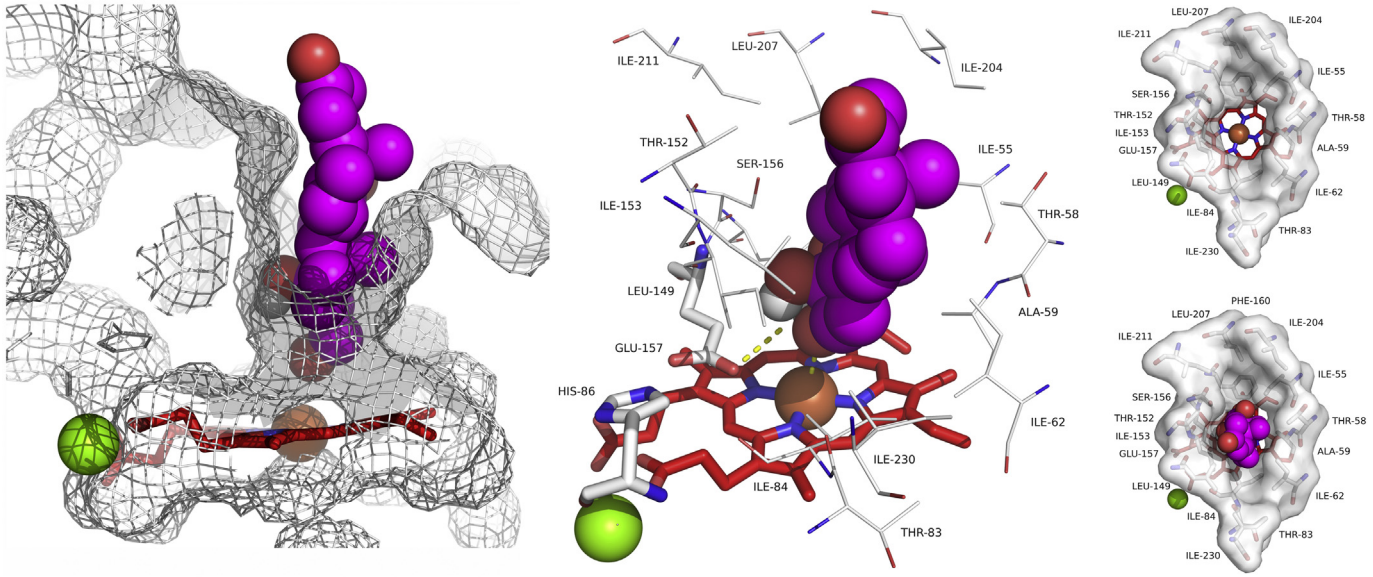


**Fig. 6.** 3D-model of *Mro*UPO when harboring cortisone (S I, in magenta) as substrate (*Mro*UPO-cortisone complex). Left side: intersection of *Mro*UPO with bound cortisone; middle: detailed view of the substrate channel (heme access channel) including catalytic residues Glu-157 (distal acid-base catalyst) and His-86 (charge stabilizer). Polar contacts of the hydroxyl group at C21 of cortisone are shown as yellow dashed lines; right side: top view of the substrate channel with and without bound cortisone (all residues forming the substrate channel are depicted and labeled). For convenience of the reader, the stabilizing magnesium ion (green ball) is shown in all views.

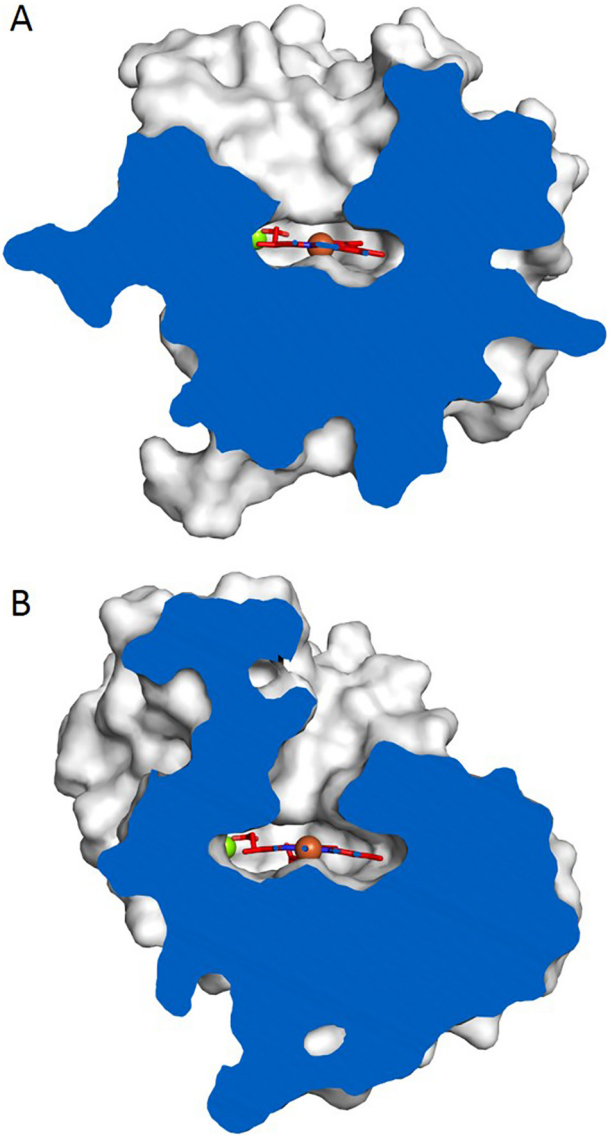


**Fig. 7.** Tangential cross sections through crystal structure-based 3D-models of *Mro*UPO and *Aae*UPO; the former (A) has a rather open and symmetric frustum-like heme access channel whereas that of the latter (B) is narrower and "carafe-shaped".

and final deacylation of cortisone-and related substrates (S I–III) by *Mro*UPO (and respectively by *Mwe*UPO) can be described as follows. In the first step, the enzymes hydroxylates the position C21 in the side chain by means of $H_2O_2$ (peroxygenation) resulting in the formation of P I that is a geminal alcohol (21-*gem*-diol, aldehyde hydrate) being in equilibrium with the corresponding free aldehyde (cortisone 21-al, P Ia) (Fig. 8). A similar reaction was observed during the oxidation of 5-hydroxymethylfurfural (HMF) by *Aae*UPO (or aryl alcohol oxidase) leading to the corresponding dialdehyde (diformylfurane), about 50% of which was in equilibrium with its stable hydrate (*gem*-diol detectable by MS) [32,33].

In the next step, the *Marasmius* UPOs catalyze a second hydroxylation leading to the corresponding α-ketocarboxylic acid P II (corstisone 21-oic acid). However, so evident the structure of P II is (compare respective NMR data), so uncertain is the exact point of enzymatic attack at P I. This is due to the different tautomeric and hydrated forms of P I. Theoretically – in addition to P I and P Ia (the latter detected by NMR, Table S2) – two further tautomeric structures, a 21-endiol and an α-hydroxy-21-oic acid, are conceivable; all of them would be substrates of *Marasmius* UPOs and converted into P II. In our opinion, the most probable route may proceed via the hydroxylation of the free aldehyde (P Ia; Fig. 8). This reaction type via abstraction of hydrogen (C-H abstraction) and OH-rebound has been reported for various UPO substrates including aromatic (e.g. benzaldehyde) and aliphatic (*n*-alkanals) aldehydes, which are oxidized into the corresponding carboxylic acids (e.g. benzoic acid and *n*-alkanoicfatty acids, respectively) [34,35]. An alternative route may start from the 21-*gem*-diol and proceed via an additional hydroxylation at C21 to form a putative 21-*gem*-triol that spontaneously dehydrates under formation of the 21-oic acid, Fig. 8). A third variant may follow the hydroxylation of the α-hydroxy-21-oic acid tautomer of P I to give the corresponding 20-*gem*-diol that dehydrates to P II; eventually, the epoxidation of the tautomeric 21-enediol could contribute to P I conversion as well (not shown). Corticosterone with the same hydroxyacetyl moiety as cortisone (but lacking OH at C17) was reported to be analogously oxidized by a panel of liver CYPs (especially of the CYP3A and CYP4A subfamilies), involving 21-*gem*-diol, 21-*gem*-triol and 21-al intermediates and resulting in the final formation of the corresponding 21-oic acid [36].

The last step in the conversion of corticosteroids by *Marasmius* UPOs proceeds via the removal of the side chain, which results, in the case of P II, in the appearance of adrenosterone (17-one, P III) (Fig. 9). Although the formation of the latter compound was unambiguously demonstrated (by an authentic standard), it is the most difficult-to-explain step of the reaction sequence [37] (Fig. 9). Taking into consideration the existing knowledge on steroidal side-chain removal by 17α-hydroxylase/C17,20-lyase (CYP17A1) [8], recently described UPO-catalyzed fatty acid decarboxylation [21] and existing knowledge on chemical decarboxylation of α-ketoacids by hydrogen peroxide [38,39], it appears to be plausible that P II undergoes both enzymatic and chemical oxidation in the course of side-chain removal (Fig. 9). Thus, a lyase-like reaction resulting in C—C bond scission between C17 and C20, release of glyoxylic acid (that is immediately oxidized/cleaved by UPO to formic acid and $CO_2$/carbonic acid) and the formation of a new double bond at C17 (carbonyl, P III) is as conceivable as the peroxide-driven oxidation of P II (caused by the peroxo-anion/$HOO^-$ at the pH used [38]), which results via a peroxo-intermediate in the release of $CO_2$ and a C17-ol/C17-oic acid derivative (P IV, the mass of which fits to the detected *m/z* [$H^+$] of 347); in a final spontaneous step, less stable P IV may decay to formic acid and P III (17-one) (Fig. 9). Whether a compound-0-like UPO-intermediate (i.e. a bound peroxo-anion-heme species) is involved as proposed for the C17,20-lyase reaction of CYP17A1 remains unclear [40]. The rapid inactivation of *Marasmius* UPOs during the obviously unfavorable conversion of P II into P III may support this assumption (Fig. 2).

The presence of equimolar amounts of magnesium ($Mg^{2+}$) in purified *Mro*UPO confirms the importance of this metal as structural element in UPO proteins. Strong indication of its presence were also found in the crystal structure of *Aae*UPO and it was detected by ICP-MS/OES analysis in highly pure preparations of the enzyme [18]. It may stabilize the porphyrin ring system that is under permanent ring strain. Interestingly, the Mg ion sits at the same position as $Mn^{2+}$ in manganese peroxidase (MnP, EC 1.11.13.1) [41]. In both cases, the metals are chelated by conserved acidic amino acid residues (Glu, Asp) and the heme propionate [18,41]. The presence of manganese was proposed for CPO based on its crystal structure (but without appropriate metal analysis) [26]. However, when considering the function of Mn in MnP [42] and the almost identical covalent atomic radiuses of $Mn^{2+}$ (1.39 Å) and $Mg^{2+}$ (1.41 Å) [43], it is more conceivable that redox-inactive $Mg^{2+}$ is present in CPO representing a halide-oxidizing UPO [14].

## 5. Conclusions

After recently reported fatty acid shortening by *Mro*UPO [21], steroidal side-chain removal is the second example of a C-C cleaving

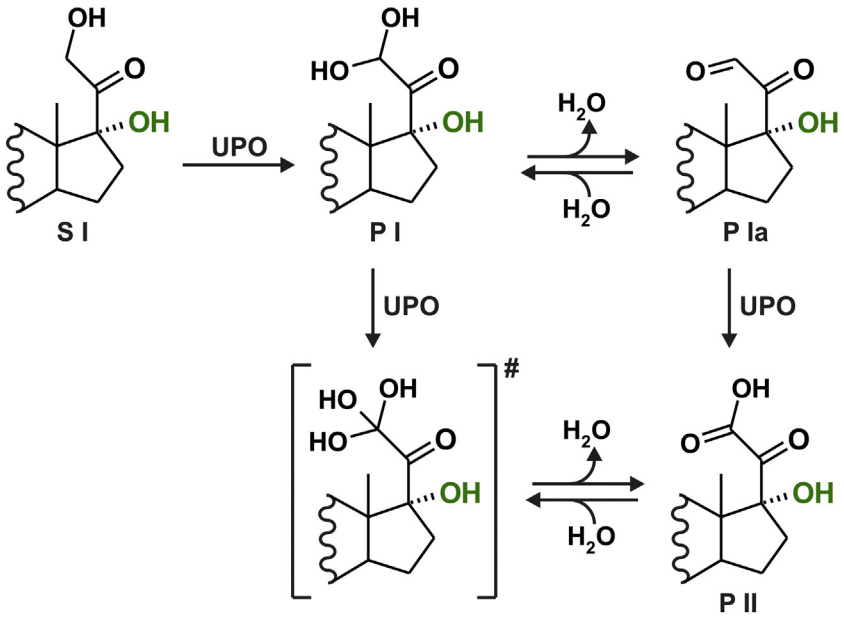


**Fig. 8.** Postulated reactions involved in the side chain oxidation of S I (cortisone) by *Mro*UPO and *Mwe*UPO. First hydroxylation at C21 results in P I (cortisone 21-*gem*-diol, identified by NMR) that is in equilibrium with the corresponding free aldehyde P Ia (cortisone 21-al, also identified by NMR). Both P I and P Ia can be subject of a second hydroxylation at C21 resulting in the direct formation of P II (cortisone 21-oic acid, detected by NMR) or in putative cortisone *gem*-triol[#] that is in equilibrium with P II.

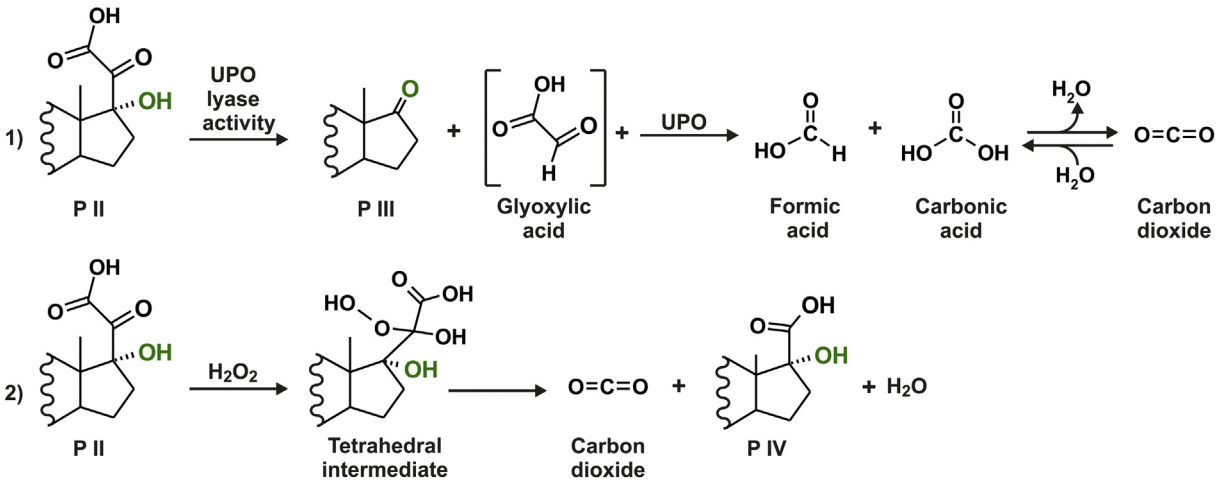


**Fig. 9.** Possible reaction sequences explaining the side chain removal from P II (cortisone 21-oic acid) by *Mro*UPO and *Mwe*UPO. 1) A lyase-like activity of UPO similar to that described in [44] may cleave the C–C bond between C17 and C20 resulting in P III (adrenosterone, identified by an authentic standard) and putative glyoxylic acid that can be cleaved by UPO into formic acid and carbonic acid/carbon dioxide (as demonstrated by authentic standards and barium carbonate precipitation). 2) P II may also chemically react with $H_2O_2$ to form a tetrahedral intermediate [38] that decomposes to carbon dioxide and P IV (17-hydroxy-3,11-dioxoandrost-4-ene-17-carboxylic acid, as indicated by mass data).

reaction (deacylation) catalyzed by this enzyme type. Thereby another prototypical reaction of P450s (in this case lyase-activity of CYP17A1) with physiological and biotechnological relevance could be ascertained for a secreted fungal peroxygenase. Future studies will have to elucidate the role of UPO compound 0 and whether other fungal UPOs (of which > 4000 sequences are known so far) may catalyze similar reactions without loosing their activity during the scission process.

## Abbreviations

| | |
|---|---|
| Aae | Agrocybe aegerita |
| ACN | acetonitrile |
| CPO | chloroperoxidase |
| CYP | cytochrome P450 |
| ESI | electrospray ionization |
| HPLC | high performance liquid chromatography |
| IC | ion chromatography |
| ICP-OES | inductively coupled plasma optical emission spectrometry |
| *Mro* | *Marasmius rotula* |
| *Mwe* | *Marasmius wettsteinii* |
| MS | mass spectrometry |
| NMR | nuclear magnetic resonance |
| SDS-PAGE | sodium dodecyl sulfate polyacrylamide gel electrophoresis |
| SEC | size-exclusion chromatography |
| SI | cortisone |
| SII | prednisone |
| SIII | Reichstein's substance S |
| TON | turnover number |
| UPO | unspecific peroxygenase |

## Conflicts of interest

The authors declare that they have no conflict of interest.

## Acknowledgements

We thank U. Schneider for isolating *Marasmius wettsteinii* and maintaining the Zittau Fungal Culture Collection and H. Heidenreich for performing ICP-OES and ICP-MS as well as A. Karich for the photography of *M. rotula* (graphical abstract). This work was supported by the German Ministry of Education and Research (Bundesministerium für Bildung und Forschung) within the program 'BioIndustrie 2021-Cluster Integrierte Biotechnololgie 2021' (project 0315877) and in part by the integrated European Union projects INDOX (KBBE 2013.3.3-04) and ENZOX2 (H2020-BBI-PPP-2015-2-1-720297). Ongoing sequencing and annotation of the genome of *M. wettsteinii* is supported by the AiF project PEROXYMEER (IGF 19636 BG/3).

## Appendix A. Supplementary data

Supplementary data to this article can be found online at https://doi.org/10.1016/j.jinorgbio.2018.03.011.

## References

[1] K. Bloch, Steroids 57 (1992) 378–383.
[2] W.L. Miller, R.J. Auchus, Endocr. Rev. 32 (2011) 81–151.
[3] D.E. Cane, D.A. Bochar, J. Freisen, C.V. Stauffacher, V.W. Rodwell, M. Rohmer, T. Koyama, K. Ogura, M.L. Wise, R. Croteau, T.M. Hohn, Isoprenoids Including Cartenoids and Steroids, first ed., Pergamon, Oxford, 1999.
[4] R.A. Hill, H.L.J. Makin, D.N. Kirk, G.M. Murphy, Dictionary of Steroids, first ed., Chapman and Hall/CRC, London, 1991.
[5] J.A.R. Salvador, S.M. Silvestre, V.M. Moreira, Curr. Org. Chem. 10 (2006) 2227–2257.
[6] S.B. Mahato, S. Garai, Steroids 62 (1997) 332–345.
[7] H.N. Bhatti, R.A. Khera, Steroids 77 (2012) 1267–1290.
[8] D. Porubek, Curr. Top. Med. Chem. 13 (2013) 1364–1384.
[9] L. Sedlaczek, L.L. Smith, Crit. Rev. Biotechnol. 7 (1988) 187–236.
[10] M. Hofrichter, R. Ullrich, Curr. Opin. Chem. Biol. 19 (2014) 116–125.
[11] M. Kluge, R. Ullrich, K. Scheibner, M. Hofrichter, Green Chem. 14 (2012) 440–446.
[12] Y. Ni, E. Fernández-Fueyo, A.G. Baraibar, R. Ullrich, M. Hofrichter, H. Yanase, M. Alcalde, W.J.H. van Berkel, F. Hollmann, Angew. Chem. Int. Ed. Eng. 55 (2016) 798–801.
[13] A.E.W. Horst, S. Bormann, J. Meyer, M. Steinhagen, R. Ludwig, A. Drews, M. Ansorge-Schumacher, D. Holtmann, J. Mol. Catal. B Enzym. 133 (2016) S137–S142.
[14] H. Kellner, M.J. Pecyna, M. Buchhaupt, R. Ullrich, M. Hofrichter, Genome Announc. 4 (2016) e00774-00716.
[15] X. Wang, S. Peter, M. Kinne, M. Hofrichter, J.T. Groves, J. Am. Chem. Soc. 134 (2012) 12897–12900.
[16] X. Wang, R. Ullrich, M. Hofrichter, J.T. Groves, Proc. Natl. Acad. Sci. U. S. A. 112 (2015) 3686–3691.
[17] K. Piontek, R. Ullrich, C. Liers, K. Diederichs, D.A. Plattner, M. Hofrichter, Acta Crystallogr. Sect. F 66 (2010) 693–698.
[18] K. Piontek, E. Strittmatter, R. Ullrich, G. Gröbe, M.J. Pecyna, M. Kluge, K. Scheibner, M. Hofrichter, D.A. Plattner, J. Biol. Chem. 288 (2013) 34767–34776.
[19] G. Gröbe, R. Ullrich, M.J. Pecyna, D. Kapturska, S. Friedrich, M. Hofrichter, K. Scheibner, AMB Express 1 (2011) 31.
[20] R. Ullrich, J. Nüske, K. Scheibner, J. Spantzel, M. Hofrichter, Appl. Environ. Microbiol. 70 (2004) 4575–4581.
[21] A. Olmedo, J.C. del Río, J. Kiebist, R. Ullrich, M. Hofrichter, K. Scheibner, A.T. Martínez, A. Gutiérrez, Chem. Eur. J. (2017) 16985–16989.
[22] C. Liers, M.J. Pecyna, H. Kellner, A. Worrich, H. Zorn, K.T. Steffen, M. Hofrichter, R. Ullrich, Appl. Environ. Microbiol. 97 (2013) 5839–5849.
[23] O. Trott, A.J. Olson, J. Comput. Chem. 31 (2010) 455–461.
[24] S. Kim, P.A. Thiessen, E.E. Bolton, J. Chen, G. Fu, A. Gindulyte, L. Han, J. He, S. He, B.A. Shoemaker, J. Wang, B. Yu, J. Zhang, S.H. Bryant, Nucleic Acids Res. 44 (2016) D1202–D1213.
[25] G.M. Morris, R. Huey, W. Lindstrom, M.F. Sanner, R.K. Belew, D.S. Goodsell, A.J. Olson, J. Comput. Chem. 30 (2009) 2785–2791.
[26] M. Sundaramoorthy, J. Terner, T.L. Poulos, Structure 3 (1995) 1367–1378.
[27] G. Nie, S.D. Aust, Arch. Biochem. Biophys. 337 (1997) 225–231.
[28] M. Matsubara, J. Suzuki, T. Deguchi, M. Miura, Y. Kitaoka, Appl. Environ. Microbiol. 62 (1996) 4066–4072.
[29] M. Hofrichter, H. Kellner, M.J. Pecyna, R. Ullrich, Fungal unspecific peroxygenases: heme-thiolate proteins that combine peroxidase and cytochrome P450 Properties, in: E.G. Hrycay, S.M. Bandiera (Eds.), Monooxygenase, Peroxidase and Peroxygenase Properties and Mechanisms of Cytochrome P450, Springer International Publishing, Cham, 2015, pp. 341–368.
[30] E.D. Babot, J.C. del Río, M. Cañellas, F. Sancho, F. Lucas, V. Guallar, L. Kalum, H. Lund, G. Gröbe, K. Scheibner, R. Ullrich, M. Hofrichter, A.T. Martínez, A. Gutiérrez, Appl. Environ. Microbiol. 81 (2015) 4130–4142.
[31] J. Kiebist, K.-U. Schmidtke, J. Zimmermann, H. Kellner, N. Jehmlich, R. Ullrich, D. Zänder, M. Hofrichter, K. Scheibner, Chembiochem 18 (2017) 563–569.
[32] J. Carro, P. Ferreira, L. Rodríguez, A. Prieto, A. Serrano, B. Balcells, A. Ardá, J. Jiménez-Barbero, A. Gutiérrez, R. Ullrich, M. Hofrichter, A.T. Martínez, FEBS J. 282 (2015) 3218–3229.
[33] L. Kalum, M.D. Morant, H. Lund, J. Jensen, I. Lapainaite, S.N. H., S. Pedersen, L.H. Østergaard, F. Xu, Enzymatic Oxidation of 5-hydroxymethylfurfural and Derivatives Thereof, WO 2014/015256 A2, Denmark, (2014).
[34] M. Kinne, C. Zeisig, R. Ullrich, G. Kayser, K.E. Hammel, M. Hofrichter, Biochem. Biophys. Res. Commun. 397 (2010) 18–21.
[35] A. Olmedo, C. Aranda, J.C. del Río, J. Kiebist, K. Scheibner, A.T. Martínez, A. Gutiérrez, Angew. Chem. Int. Ed. Eng. 55 (2016) 12248–12251.
[36] T. Wang, Y.M. Shah, T. Matsubara, Y. Zhen, T. Tanabe, T. Nagano, S. Fotso, K.W. Krausz, T.M. Zabriskie, J.R. Idle, F.J. Gonzalez, J. Biol. Chem. 285 (2010) 7670–7685.
[37] S. Bonomo, F.S. Jørgensen, L. Olsen, J. Chem. Inf. Model. 57 (2017) 1123–1133.
[38] E. Melzer, H.L. Schmidt, Biochem. J. 252 (1988) 913–915.
[39] B. Siegel, J. Lanphear, J. Organomet. Chem. 44 (1979) 942–946.
[40] M. Akhtar, J.N. Wright, Acyl-carbon bond cleaving cytochrome P450 enzymes: CYP17A1, CYP19A1 and CYP51A1, in: E.G. Hrycay, S.M. Bandiera (Eds.), Monooxygenase, Peroxidase and Peroxygenase Properties and Mechanisms of Cytochrome P450, Springer International Publishing, Cham, 2015, pp. 107–130.
[41] M. Sundaramoorthy, K. Kishi, M.H. Gold, T.L. Poulos, J. Biol. Chem. 269 (1994) 32759–32767.
[42] H. Wariishi, K. Valli, M.H. Gold, J. Biol. Chem. 267 (1992) 23688–23695.
[43] The periodic table of the elements, Manganese: radii of atoms and ions. https://www.webelements.com/manganese/atom_sizes.html, 2018 (accessed 5 January 2018).
[44] S. Nakajin, M. Shinoda, M. Haniu, J.E. Shively, P.F. Hall, J. Biol. Chem. 259 (1984) 3971–3976.